Materials Letters 258 (2020) 126806

Contents lists available at ScienceDirect

Materials Letters

journal homepage: www.elsevier.com/locate/mlblue

Investigation on the precipitate formation and behavior in nitrogen-containing equiatomic CoCrFeMnNi high-entropy alloy

Dennis Edgard Jodi [a], Joohyun Park [b,*], Boris Straumal [c,d,e], Nokeun Park [a,f,*]

[a] School of Materials Science and Engineering, Yeungnam University, 280 Daehak-ro, Gyeongbuk 38541, Republic of Korea
[b] Department of Materials Engineering, Hanyang University, Ansan 15588, Republic of Korea
[c] Institute of Solid State Physics and Chernogolvka Scientific Center, Russian Academy of Sciences, Chernogolvka 142432, Russia
[d] National University of Science and Technology «MISIS», Moscow 119049, Russia
[e] Karlsruhe Institute of Technology, Institute of Nanotechnology, Eggenstein-Leopoldshafen 76344, Germany
[f] Institute of Materials Technology, Yeungnam University, 280 Daehak-ro, Gyeongbuk 38541, Republic of Korea

ARTICLE INFO

Article history:
Received 26 September 2019
Received in revised form 5 October 2019
Accepted 11 October 2019
Available online 11 October 2019

Keywords:
Metals and alloys
High-entropy alloys
Nitrogen
Interstitial alloys
Microstructure
Precipitate

ABSTRACT

The precipitate formation and behavior in nitrogen-containing high-entropy alloy of equiatomic CoCrFeMnNi were characterized. The presence of 0.95 at.% nitrogen led to the formation of Cr_2N precipitate in the as-recrystallized N-CoCrFeMnNi, in which annealing temperature affected the fraction and size of the formed Cr_2N particles. It was observed that the Cr_2N exhibited a Kikuchi crystal orientation relation (OR) with the face-centered cubic (FCC) matrix, and the OR was noticed to be in the plane of $\{1\,1\,1\}\gamma//\{0\,0\,0\,1\}Cr_2N$ and direction of $\langle 1\,1\,0\rangle\gamma//\left\langle 1\,\bar{1}\,0\,0\right\rangle$ Cr_2N.

1. Introduction

The development of precipitation-induced medium- and high-entropy alloys (MEAs and HEAs) has been intensively performed recently. This exploration was taken to enhance the mechanical properties of these alloys. The mechanical properties of these systems tended to decrease in several circumstances despite to a remarkable strength-ductility balance [1]. The implementation of precipitation hardening by substitutional element addition, i.e. Al nanoprecipitate, was reported to be effective in improving the mechanical properties of MEA [2]. As for the utilization of interstitial element, it was observed that nitrogen addition led to nitride precipitate formation in HEA [3]. Considering the abundance availability and cost-effectiveness of nitrogen, it is then fascinating to investigate the effect of nitrogen addition toward the microstructure and precipitate formation in MEAs and HEAs. Herein, we investigated the precipitate formation by nitrogen addition in equiatomic CoCrFeMnNi HEA. The equiatomic CoCrFeMnNi was chosen, as aside from being widely studied HEA system, CoCrFeMnNi can maintain its face-centered cubic (FCC) phase over a wide temperature range. The investigation was also performed to observe the behavior of the formed precipitates in N-CoCrFeMnNi.

2. Experimental procedures

High-purity raw materials (Fe, Cr, Mn, Ni: >99.99 wt%; Co: >99.95 wt%) were placed in a fused alumina crucible, and then heated to 1773 K in a super kanthal vertical furnace. Nitrogen gas (ultrahigh purity, >99.999%) was then flowed for 24 h to homogenously saturate the CoCrFeMnNi with nitrogen. The molten N-CoCrFeMnNi was then water-quenched, and the ingot surface (±1 mm in depth) was ground. For comparison, N-free CoCrFeMnNi was also fabricated by an arc-melting process.

Both the ingots of N-CoCrFeMnNi and CoCrFeMnNi (referred as NC and C, respectively) were initially homogenized for 24 h at 1473 K under Ar-rich atmosphere. The nitrogen content measurement using a LECO combustion analyzer, which was performed after the specimen was ground on both surfaces by 0.25 mm, showed a nitrogen value of 0.95 at.%. This was followed by a cold-rolling with 90% thickness reduction to eliminate any as-cast structure. An annealing treatment for 1 h at different

* Corresponding authors at: Department of Materials Engineering, Hanyang University, Ansan 15588, Republic of Korea (J. Park), and School of Materials Science and Engineering, Yeungnam University, 280 Daehak-ro, Gyeongbuk 38541, Republic of Korea (N. Park).

E-mail addresses: basicity@hanyang.ac.kr (J. Park), nokeun_park@yu.ac.kr (N. Park).

https://doi.org/10.1016/j.matlet.2019.126806
0167-577X/

temperatures of 873 K (NC873, C873) 973 K (NC973, C973), 1073 K (NC1073, C1073), 1173 K (NC1173, C1173), and 1273 K (NC1273, C1273) was then performed to obtain recrystallized structure, and all specimens were water-quenched subsequently.

Prior to microstructural observation, all specimens were ground using SiC papers, followed by electropolishing with a mixed solution of 90% acetic acid +10% perchloric acid. The initial microstructural observation was performed using a field-emission scanning electron microscope (FE-SEM) in backscatter electron (BSE) mode. A transmission electron microscope (TEM) was utilized to analyze the formed precipitates. The disk-shaped specimen of 3 mm in diameter was prepared using a twin-jet polisher. Further microstructural observation was performed using an FE-SEM equipped with electron back-scattered diffraction (SEM-EBSD) detector.

For the thermodynamic calculations, FactSage™ (ver. 7.1) software with integrated databases of FactPS and FSstel was utilized. The FactPS database includes the thermodynamic information of nitrogen gaseous elements. A Scheil-Gulliver simulation was used to calculate the precipitation behavior during cooling to simulate the actual precipitation behavior in $N_{0.95}$-CoCrFeMnNi. This thermodynamic prediction method has been successfully utilized to simulate the precipitation behavior in CoCrFeMnNi in our previous study [4].

3. Results and discussion

Initial microstructure observation showed a deformed structure from the cold-rolling process in NC873, which suggests that 873 K is too low for recrystallization in $N_{0.95}$-CoCrFeMnNi (Fig. 1a). With higher annealing temperature between 973 and 1173 K, the microstructure displayed recrystallized structures with fine grain size and secondary precipitates formation (Fig. 1b–d). In NC1273, recrystallized structure with significantly coarser grains and numerous recrystallization twins was observed (Fig. 1e). However, no presence of precipitates was observed by SEM-BSE in NC1273, suggesting that annealing temperature affects the precipitate formation in $N_{0.95}$-CoCrFeMnNi.

TEM-energy dispersive spectroscopy (EDS) mapping taken from dark-field (DF) image in Fig. 2a displayed a high Cr and N content in the precipitates (Fig. 2b–g). Fast-Fourier transform (FFT) image (Fig. 2h) confirms that this precipitate is a Cr_2N trigonal phase. Here, aside from the low Gibbs free energy (ΔG_f) of Cr-N compared to other nitride [unpublished work], a high solubility and strong affinity of N with Cr was also exhibited causing the formation of Cr-N nitride to be preferred compared to other nitride [5]. As for Cr_2N, due to the lower ΔG_f of Cr_2N than CrN, the formation of Cr_2N is thus more favorable than CrN [6].

By employing SEM-EBSD, it was observed that the matrix of all studied $N_{0.95}$-CoCrFeMnNi specimens maintained the FCC phase. SEM-EBSD also revealed a very small fraction of Cr_2N in NC1273 [data not shown]. It was further observed that Cr_2N exhibited a crystal orientation relation (OR) with one facet of the FCC matrix (Fig. 2i–k). The OR was observed to be on-plane of $\{1\,1\,1\}\gamma // \{0\,0\,0\,1\}Cr_2N$ and direction of $\langle 1\,1\,0\rangle\gamma // \left\langle 1\,\bar{1}\,0\,0\right\rangle Cr_2N$, which is similar to the previously studied Kikuchi crystal OR [6,7]. Since only one facet exhibited an OR (Cr_2N-FCC 1 facet), it could be concluded that Cr_2N was partially coherent with the matrix. The semi-coherency of Cr_2N-FCC helped to lower the minimum activation energy barrier and the interface energy for the Cr_2N formation along the FCC matrix grain boundary, which is also suggested from the occurrence of wetting phenomenon displayed in Fig. 2i [6,8].

Here, annealing temperature affects the Cr_2N formation in $N_{0.95}$-CoCrFeMnNi. In lower annealing temperature, high fraction of fine-sized Cr_2N was formed (Fig. 3a). Meanwhile, at higher temperature, the Cr_2N fraction was lessened followed by the precipitates coarsening. The Scheil-Gulliver modeling (Fig. 3b) predicts that initially FCC phase will form as the main matrix. The Cr_2N is then predicted to form below 1500 K and it reached a maximum

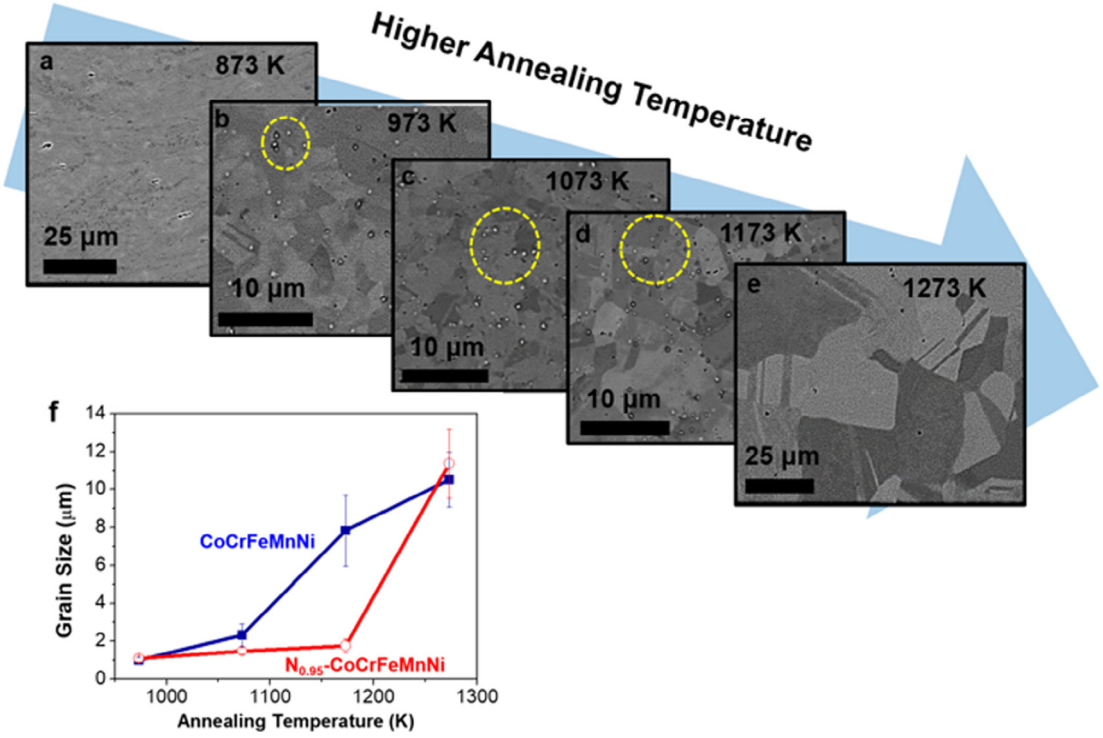

Fig. 1. SEM-BSE observation on (a) NC873, (b) NC973, (c) NC1073, (d) NC1173, and (e) NC1273; (f) Grain size comparison between the as-recrystallized $N_{0.95}$-CoCrFeMnNi and CoCrFeMnNi.

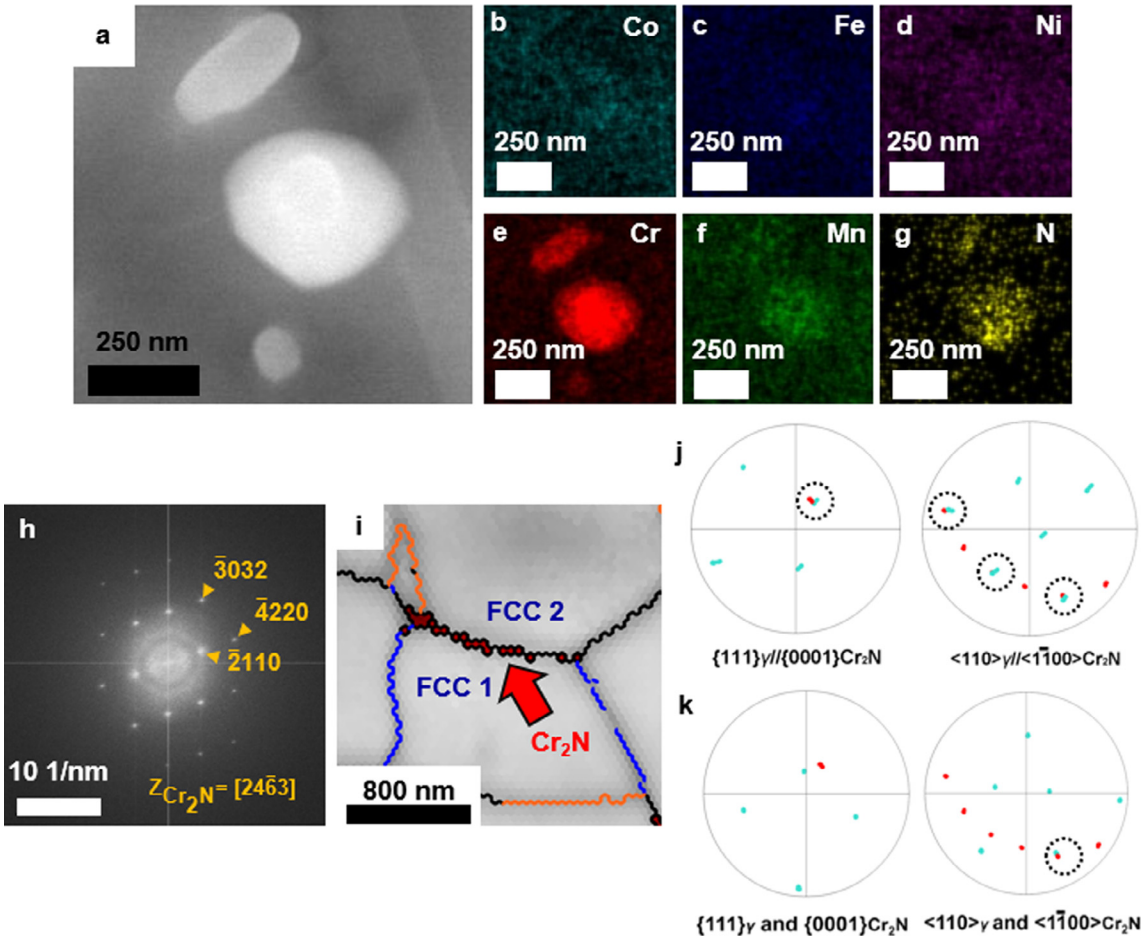

Fig. 2. TEM observation on NC1073. (a) DF observation; (b–g) TEM-EDS mapping from (a) of each constituent in $N_{0.95}$-CoCrFeMnNi; (h) FFT pattern of the precipitate; (i) SEM-EBSD image quality map of NC1173, showing crystal orientation between the Cr_2N and the FCC matrix at point (j) 1 and (k) 2.

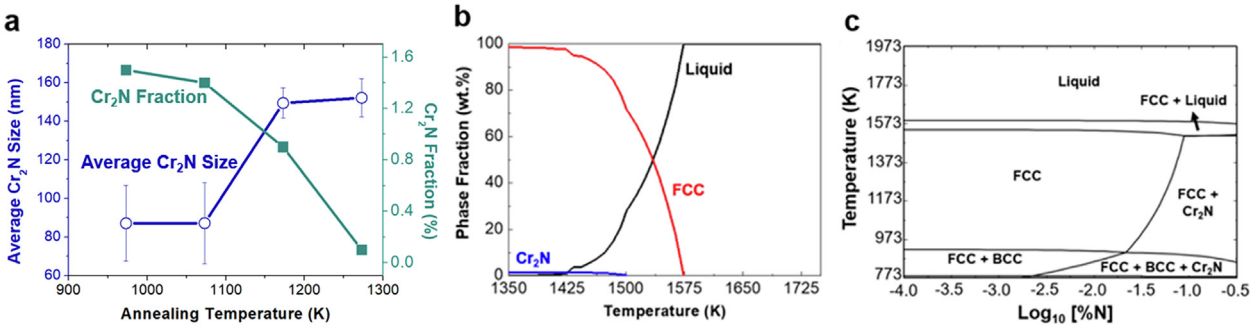

Fig. 3. (a) Cr_2N size and fraction with different annealing temperature; (b) Scheil-Gulliver model for the formation of Cr_2N during cooling in $N_{0.95}$-CoCrFeMnNi; (c) theoretical phase diagram of N_x-CoCrFeMnNi.

fraction of 1.44 wt%. This prediction was different from the actual result, in which the Cr_2N fraction tended to decrease with higher annealing temperature. The lower Cr_2N fraction in higher annealing temperature can be justified by predicting the phase stability between FCC and Cr_2N using the N-CoCrFeMnNi phase diagram (Fig. 3c). The FCC matrix becomes more stable in higher temperature, which was indicated by the change of FCC solvus line in the phase diagram of N-CoCrFeMnNi. It can be thus predicted that the formation of FCC matrix is preferable than Cr_2N in higher temperature. Moreover, considering that the ΔG_f for Cr_2N tends to increase with higher temperature, this further explains the reason behind less Cr_2N formation in this study [6].

Further discussion is then performed to analyze the Cr_2N effect on grain growth in $N_{0.95}$-CoCrFeMnNi. Since the Cr_2N exhibited an OR with the FCC matrix, a Zener pinning pressure (P_z) might occur that affects the grain growth and resulting grain size of the as-recrystallized $N_{0.95}$-CoCrFeMnNi [9]. The P_z is influenced by the precipitate average size and fraction. Theoretically, high fraction, fine-sized precipitates would lead to high P_z, which cause high grain growth hindrance and fine grain size formation. Meanwhile, low fraction, coarse-sized precipitates will result in low P_z, causing coarser grains to form.

Here, NC973 exhibited the highest fraction of fine-sized Cr_2N, which theoretically led to a high P_z and the formation of fine grain

size. In this case, NC973 exhibited a similar grain size as C973. This occurred since C973 also exhibited the formation of σ-phase precipitate (data not shown), in which σ-phase was reported to exhibited an OR with the FCC matrix [10]. This caused the C973 to also exhibit P_z by σ-phase, causing a similar grain size formation as NC973. With increasing annealing temperature, the Cr_2N size was becoming coarser with lesser fraction, causing lower P_z and coarser grain sizes formation. In this case, the CoCrFeMnNi specimens exhibit no formation of σ-phase, and it can be clearly observed that the P_z caused NC1073 and NC1173 to exhibit finer grains compared to that of C1073 and C1173. Meanwhile, in NC1273, since only a tiny fraction of coarse-sized Cr_2N is present, the P_z contribution could be neglected. This caused the grains in NC1273 to be significantly coarser compared to other $N_{0.95}$-CoCrFeMnNi specimens and caused also the formation of a similar grain size as C1273.

The Cr_2N formation with different size and fraction with different annealing temperature opens the possibility for further exploration in combining the most appropriate microstructure with the desired mechanical properties. Further study will then be performed to optimize the nitrogen addition toward mechanical properties enhancement in MEAs and HEAs.

4. Conclusions

The precipitates formation and behavior in N-CoCrFeMnNi were successfully characterized. The presence of 0.95 at.% nitrogen caused the Cr_2N precipitate formation in the as-recrystallized $N_{0.95}$-CoCrFeMnNi. The Cr_2N exhibited a Kikuchi crystal orientation relation (OR) with the face-centered cubic (FCC) matrix in the plane of $\{1\,1\,1\}\gamma//\{0001\}Cr_2N$ and direction of $\langle 1\,1\,0\rangle\gamma//\left\langle 1\,\bar{1}\,0\,0\right\rangle Cr_2N$. The size and fraction of the Cr_2N was affected by the annealing temperature, which subsequently led to different Zener pinning pressure and affected the grain size of the as-recrystallized $N_{0.95}$-CoCrFeMnNi.

Declaration of Competing Interest

The authors declare that they have no known competing financial interests or personal relationships that could have appeared to influence the work reported in this paper.

Acknowledgment

This research was supported by the Basic Science Research Program through the National Research Foundation of Korea (NRF) funded by the Ministry of Education (Grant number NRF-2018R1A2B6005809). It was also partially supported by the Ministry of Education and Science of the Russian Federation in the framework of the Program to Increase the Competitiveness of NUST "MISiS" and the state tasks of ISSP RAS and CSC RAS (Straumal).

Appendix A. Supplementary data

Supplementary data to this article can be found online at https://doi.org/10.1016/j.matlet.2019.126806.

References

[1] C. Yang, K. Aoyagi, H. Bian, A. Chiba, Mater. Lett. 254 (2019) 46–49.
[2] D. Lee, H.U. Jeong, K.H. Lee, J.B. Jeon, N. Park, Mater. Lett. 250 (2019) 127–130.
[3] W. Wang, S. Song, K.M. Reddy, W. Li, P. Liu, X. Wang, Mater. Lett. 255 (2019) 126566.
[4] N. Choi, K.R. Lim, Y.S. Na, U. Glatzel, J.H. Park, J. Alloys Compd. 763 (2018) 546–557.
[5] C. Kowanda, M.O. Speidel, Scr. Mater. 48 (2003) 1073–1078.
[6] D.E. Jodi, J.H. Park, N. Park, Mater. Charact. 157 (2019) 109888.
[7] T. Tanaka, M. Kikuchi, R. Tanaka, J. Japan Inst. Met. Mater. 41 (1977) 1145–1153.
[8] A.B. Straumal, B.S. Bokstein, A.L. Petelin, B.B. Straumal, B. Baretzky, A.O. Rodin, A.N. Nekrasov, J. Mater. Sci. 47 (2012) 8336–8343.
[9] F.J. Humphreys, M. Hatherly, Recrystallization and Related Annealing Phenomena: 2nd Edition, 2004.
[10] G. Laplanche, S. Berglund, C. Reinhart, A. Kostka, F. Fox, E.P. George, Acta Mater. 161 (2018) 338–351.